

QCD PREDICTIONS FOR $\gamma\gamma$ ANNIHILATION TO BARYONS

Glennys R. FARRAR*, Ezio MAINA** and Filippo NERI***

*Department of Physics and Astronomy, Rutgers University,
New Brunswick, New Jersey 08903, USA*

Received 30 May 1984
(Revised 14 March 1985)

QCD predictions for large-momentum transfer cross sections of the type $\gamma\gamma \rightarrow B\bar{B}'$ are given, for B and B' any members of the baryon octet or decuplet, and all possible helicity combinations for photons and baryons.

1. Introduction

Thanks to the increased luminosity of high-energy e^+e^- colliders, measurements of $\gamma\gamma \rightarrow$ baryon-antibaryon at large-momentum transfer have finally become feasible [1–3]. For sufficiently large momentum transfer (possibly $t \geq 5 \text{ GeV}^2$), perturbative QCD in the Born approximation is supposed to correctly and completely predict these cross-sections, including their energy, angular, and polarization dependence, and their absolute normalization [4, 5]. The $\gamma\gamma \rightarrow B\bar{B}'$ reactions have a special role in testing perturbative QCD applied to exclusive scattering reactions: only $\gamma\gamma \rightarrow$ hadron-antihadron, and elastic form factors, are free of propagator singularities and the still-poorly-understood Sudakov suppression. Thus $\gamma\gamma \rightarrow B\bar{B}'$ may be the most complicated process that can be expected to be reliably predictable, at sufficiently large t , using only the QCD Born approximation. Moreover it has been shown in ref. [6] how to use comparisons between various $\gamma\gamma \rightarrow B\bar{B}'$ reactions to independently check whether the experiments are actually at sufficiently large-momentum transfer that the perturbative QCD predictions should be reliable.

We have undertaken to obtain the leading QCD predictions for all large p_t exclusive hadron scattering processes, including photoproduction, meson-nucleon scattering, pN annihilation, and nucleon-nucleon scattering. The first step in this effort [7] was to develop a method for analytically evaluating, by a specially designed

* John Simon Guggenheim Memorial Foundation Fellow. Supported in part by the National Science Foundation, grant number NSF-PHY-84-15534.

** Work partially supported by the University of Torino and Foundation Angelo Della Riccia.

*** Current address: Physics Dept., University of Maryland, College Park, Maryland.

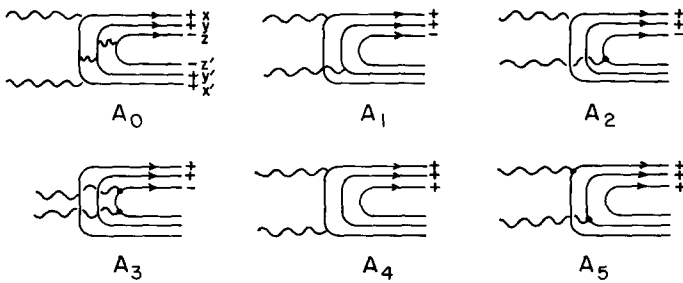


Fig. 1. Independent quark amplitudes necessary to completely determine $\gamma\gamma \rightarrow B_8 \bar{B}_8$, $B_8 \bar{B}_{10}$, and $B_{10} \bar{B}_{10}$, with photon symmetrization and gluon connections understood. The + (-) labels the chirality of the fermion line.

algebraic computer program, the enormous number of non-trivial quark scattering diagrams which are needed even in the Born approximation. (For instance pp scattering involves eight distinct 6-quark scattering amplitudes, each of which is the sum of roughly 60 000 $O(\alpha^5)$ Feynman diagrams!) A by-product of this effort is that we are easily able to perform the calculations necessary to predict the cross sections for $\gamma\gamma$ annihilations to any pair of octet or decuplet baryons, separately for each distinguishable photon and baryon helicity state. We present these results here, leaving a description of the technical aspects of the computer calculation to future publications. The unpolarized $\gamma\gamma \rightarrow p\bar{p}$ cross section has been previously calculated by Damgaard [8], however we disagree with his results as discussed in sect. 5. A subset of our results have appeared earlier: the fixed α_s calculations in ref. [9], and the running coupling constant calculations with symmetric wave functions in ref. [10].

2. Calculation

Fig. 1 shows the fundamental quark amplitudes which must be computed in the Born approximation. Each graph of fig. 1 is to be understood as a sum of diagrams with the photons interchanged and with the two gluons connected in all possible ways. Quark masses are neglected, so that each quark line can be labeled by its chirality and momentum fraction. Diagrams containing trilinear gluon vertices vanish identically when projected onto the color singlet baryons. Thus amplitudes A_0 , A_3 and A_4 of fig. 1 each involve a sum of 48 diagrams, and A_1 , A_2 and A_5 , a sum of 68 diagrams. The analytic evaluation of these is accomplished by computer, using techniques described in ref. [7]. The analytic method introduced in ref. [7] is so powerful that, employing it, $\gamma\gamma \rightarrow B\bar{B}$ diagrams are not very difficult, and we have evaluated about 100 diagrams in Feynman gauge by hand to check our computer program. The computer program evaluates the diagrams in arbitrary covariant

gauges for SU(3) and U(1). The gauge invariance of the full amplitude is a very powerful check of its correctness. We have also checked that our computer's results agree with all other correct calculations of exclusive reactions for which explicit analytic amplitudes are available in the literature, namely $\gamma\gamma \rightarrow \pi\pi$, $\rho\rho$ [11], and the pion [12] and nucleon [4] form factors.

To evaluate the amplitude for production of physical baryons, the fundamental quark amplitudes A_{0-5} must be integrated over the wave functions giving the amplitude for the quarks to carry momentum fractions x, y, z and x', y', z' inside the baryons. Asymptotically, for infinite momentum transfer, these wave functions are [4] $(xyz)\delta(x+y+z-1)$, times the SU(6) flavor wave function and an overall normalization factor, ϕ_B . Given the wave function at one value of q^2 , QCD in principle determines it at all other q^2 's. For instance, the coefficient of the leading asymptotic term xyz decreases as $(\ln(q^2/\Lambda^2))^{-2/3\beta}$ for helicity $-\frac{1}{2}$ baryons and as $(\ln(q^2/\Lambda^2))^{-2/8}$ for helicity $\pm\frac{3}{2}$ [4]*. Just as in any QCD calculation involving $\alpha_s \sim \ln^{-1}(q^2/\Lambda^2)$, a next-higher-order calculation must be done in order to determine the value of Λ appropriate for the particular process, in terms of a standard value such as $\Lambda_{\overline{\text{MS}}}$.

Since present experiments may not be at high enough momentum transfer that the asymptotic form of the wave function is valid, and to determine the sensitivity of the predictions to the form of the wave function, we evaluate the cross section predictions for two extreme choices for the wave functions, the asymptotic form $xyz\delta(x+y+z-1)$ and the "non-relativistic" equipartition form $\delta(x-\frac{1}{3})\delta(y-\frac{1}{3})\delta(z-\frac{1}{3})$, as well as for an intermediate form $(xyz)^2\delta(x+y+z-1)$. In addition, for $\gamma\gamma \rightarrow p\bar{p}$ and $\gamma\gamma \rightarrow n\bar{n}$, results using the wave function proposed by Chernyak and Zhitnitsky [13] derived from QCD sum rules are given in sect. 3 below. We also do the calculation with both fixed and running coupling constants. In the latter case a gluon of 4-momentum k^2 has associated with it

$$\alpha_s(k^2) = \frac{4\pi}{\beta_0 \ln(k^2/c_1 s) + (\beta_1/\beta_0) \ln \ln(k^2/c_1 s)}$$

for $\alpha_s \leq c_2$ and $\alpha_s = c_2$ otherwise. (In the following, $c_2 = 1$ unless specified otherwise.) We have checked the sensitivity of our predictions to Λ and the renormalization scheme by taking several choices of c_1 , generally 1.6×10^{-3} and 6.4×10^{-3} . For the renormalization scheme advocated in ref. [14] and $s = 25 \text{ GeV}^2$, these two values of c_1 correspond to $\Lambda = 0.1$ and 0.2 GeV , or at $s = 10 \text{ GeV}^2$, to $\Lambda = 0.06$ and 0.17 GeV .

The $\gamma\gamma \rightarrow B\bar{B}$ cross sections contain the factor $[\phi_B^2]^2$. So does the cross section for $\psi \rightarrow B\bar{B}$, which is also calculable in perturbative QCD. By comparing the ratio of

* In the following we neglect this overall q^2 dependence of the wave function because in practice it is unimportant in the kinematic range of the experiments and is easily included by a reader who is interested in a substantially different q^2 regime.

TABLE 1
 ϕ_B^2 for various choices of wave function and α_s behavior

α_s choice	Wave function choice		Equipartition
	(xyz)	$(xyz)^2$	
fixed = 0.2	1.49E - 01	5.40E + 02	5.06E - 05
fixed = 0.183	1.96E - 01	7.02E + 2	6.60E - 05
α_s fixed = 0.183 on charmed quark only:			
$c_1 = 1.6E - 03$	7.90E - 02	3.80E + 02	4.41E - 05
$c_1 = 6.4E - 03$	4.28E - 02	1.92E + 02	2.50E - 05

(xyz) denotes $\psi = \phi_B xyz \delta(1 - x - y - z)$, $(xyz)^2$ denotes $\psi = \phi_B (xyz)^2 \delta(1 - x - y - z)$, and equipartition denotes $\psi = \phi_B \delta(x - \frac{1}{3}) \delta(y - \frac{1}{3}) \delta(z - \frac{1}{3})$.

branching ratios $\text{br}(\psi \rightarrow p\bar{p})/\text{br}(\psi \rightarrow e^+e^-)$ we determine ϕ_p at $s = m_\psi^2$ for a given choice of α_s and form of the baryon wave function. Normalizing the flavor and color parts of the baryon wave functions to 1, and neglecting the proton mass*, the result is

$$\begin{aligned} \frac{\text{amp}(\psi \rightarrow p\bar{p})}{\text{amp}(\psi \rightarrow e^+e^-)} &= \left[\frac{1}{2} m_\psi \right]^{-4} \frac{5}{36} \int_0^1 dx \int_0^{1-x} dy \int_0^1 dx' \int_0^{1-x'} dy' \\ &\times \frac{g^6}{e^2} \frac{\phi_B^2 xyzx'y'z' [xy' + x'y]}{xyzx'y'z' [y(1-y') + y'(1-y)] [x(1-x') + x'(1-x)]} \end{aligned}$$

for the asymptotic wave function and fixed α_s , to be definite. When doing the calculation with running couplings we replace the g^3 from the gluon attachments to the charmed quark by $[4\pi(0.18)]^{3/2}$ (i.e. $\alpha_s = 0.18$), and the g^3 from the gluon attachments to light quarks by $[(4\pi)^3 \alpha_s (xx'm_\psi^2) \alpha_s (yy'm_\psi^2) \alpha_s (zz'm_\psi^2)]^{1/2}$, since the 4-momentum squared of the gluon attached to the i th quark is $x_i x'_i m_\psi^2$. Using $\text{br}(\psi \rightarrow p\bar{p}) = 0.0022 \pm 0.0002$ and $\text{br}(\psi \rightarrow e^+e^-) = 0.074 \pm 0.012$ yields the normalization factors given in table 1**.

The final step in computing the amplitudes for producing physical baryons is to project the fundamental amplitudes A_i onto the physical hadron SU(6) wave functions, appropriately weighted with the quark charges. Table 2 gives the amplitudes for all octet and decuplet final states in terms of A_{0-5} [6]. We assume below that all octet and decuplet wave functions have the same short-distance normalization as the proton. This is experimentally confirmed at the 20% level. [6].

* Including m_p turns out to make very little difference in the result, since its effects in the propagators and its effects via phase space tend to cancel.

** For fixed $\alpha_s = 0.2$, normalizing $\gamma\gamma \rightarrow p\bar{p}$ to $\psi \rightarrow 3$ gluons, rather than $\psi \rightarrow e^+e^-$, gives essentially the same ϕ_p [15].

TABLE 2
Amplitudes for $\gamma\gamma \rightarrow B\bar{B}'$ in terms of the fundamental quark amplitudes shown in fig. 1
(these results should be multiplied by $\frac{1}{9}$)

$\gamma\gamma \rightarrow$ final state	Coeff	A_0	A_1	A_2	A_3	A_4	A_5
$p, \bar{p} \downarrow (\Sigma^+_1 \bar{\Sigma}^-_1)$	1	7	2	-2	2		
$n, \bar{n} \downarrow (\Xi^0_1 \bar{\Xi}^0_1)$	1	3	0	-3	3		
$\Sigma^-_1 \bar{\Sigma}^-_1 (\Xi^-_1 \bar{\Xi}^-_1)$	1	2	1	2	1		
$\Lambda, \bar{\Lambda}_\downarrow$	$\frac{1}{2}$	7	-1	-5	5		
$\Sigma^0_1 \bar{\Sigma}^0_1$	$\frac{1}{2}$	9	-3	-3	3		
$\Lambda, \bar{\Sigma}^0_\downarrow$	$\frac{1}{2}\sqrt{3}$	-1	1	-1	1		
$n, \bar{\Delta}^0_1 (\Xi^0_1 \bar{\Xi}^{*0}_1)$	$\sqrt{2}$	-1	1	-1	1		
$\Lambda, \bar{Y}^{*0}_\downarrow$	$\sqrt{\frac{1}{2}}\sqrt{3}$	-1	1	-1	1		
$\Sigma^0_1 \bar{Y}^{*0}_\downarrow$	$\frac{1}{2}$	-1	1	-1	1		
$p, \bar{\Delta}^+_1 (\Sigma^+_1 \bar{Y}^{*+}_1)$	$\sqrt{2}$	1	2	-2	-1		
$\Delta^{++}_{1/2} \bar{\Delta}^{++}_{3/2}$	4					3	3
$\Delta^{++}_1 \bar{\Delta}^{++}_\downarrow$	4	2	1	1	1		
$\Delta^+_{1/2} \bar{\Delta}^+_{3/2}$	1					9	0
$\Delta^+_1 \bar{\Delta}^+_\downarrow$	1	6	0	0	3		
$\Delta^0_{1/2} \bar{\Delta}^0_{3/2}$	1					6	-3
$\Delta^0_1 \bar{\Delta}^0_\downarrow$	1	4	-1	-2	1		

In the limit that quark masses can be neglected, QCD and QED conserve chirality. This requires the baryon and antibaryon to have opposite helicities: they have the same chirality and the chirality is the negative of the helicity for an antiquark. Thus the distinct final states are $(\pm \frac{1}{2}, \mp \frac{1}{2})$ and $(\pm \frac{3}{2}, \mp \frac{3}{2})$. However there are only four independent helicity-polarization combinations, say $RR \rightarrow (+\frac{1}{2}, -\frac{1}{2})$, $RR \rightarrow (+\frac{3}{2}, -\frac{3}{2})$, $RL \rightarrow (+\frac{1}{2}, -\frac{1}{2})$ and $RL \rightarrow (+\frac{3}{2}, -\frac{3}{2})$. All others are obtained from these by using rotation, charge conjugation, and parity invariance, so that $|LL \rightarrow (\lambda_1, \lambda_2)| = |LL \rightarrow (-\lambda_1, -\lambda_2)| = |RR \rightarrow (\lambda_1, \lambda_2)| = |RR \rightarrow (-\lambda_1, -\lambda_2)|$ and $|LR \rightarrow (\lambda_1, \lambda_2)(\theta)| = |RL \rightarrow (\lambda_1, \lambda_2)(\pi - \theta)| = |RL \rightarrow (-\lambda_1, -\lambda_2)(\theta)| = |LR \rightarrow (-\lambda_1, -\lambda_2)(\pi - \theta)|$. The flavor projection is independent of which of the B and B' is the antibaryon so that, e.g. $[\gamma_1 \gamma_2 \rightarrow \Sigma^- \bar{\Delta}^+] = [\gamma_1 \gamma_2 \rightarrow \Delta^+ \bar{\Sigma}^-]$, as required by C -invariance.

The results of the calculation outlined above are given in table 3. This consists of a tabulation of the predicted values of the A_{0-5}^{RR} and A_{0-5}^{RL} , as a function of $\cos \theta^*$,

* Defined to be the angle between the initial γ_R and the final baryon; clearly RR (LL) must be symmetric in $\cos \theta^*$.

under the various combinations of assumptions for wave function and coupling constant behavior considered in table 1. Weighting these amplitudes with the coefficients in table 2 and the appropriate ϕ_B^2 from table 1 gives any hadronic amplitude desired. The unpolarized cross sections are then

$$s^6 \frac{d\sigma}{dt} = \frac{1}{16\pi} (0.389 \times 10^6 \text{ nb} \cdot \text{GeV}^2) [\phi_B^2]^2 \sum_{\substack{\text{final} \\ \text{helicities}}} \frac{1}{4} \sum_{\substack{\text{initial} \\ \text{helicities}}} |\text{amp}|^2.$$

For $\gamma\gamma \rightarrow p\bar{p}$ the unpolarized cross sections are tabulated in Table 4.

An unanticipated result of our computer calculation was that the amplitudes for $\gamma_R\gamma_R \rightarrow B_{\pm 3/2}\bar{B}'_{\mp 3/2}$ vanish identically, diagram by diagram. The vanishing of these amplitudes is not the result of a symmetry (at $\theta \neq 0, \pi$), and, as shown in [6], persists at every order of perturbation theory as long as quark masses and p_t 's can be neglected. Thus measuring $\gamma_R\gamma_R$ (and/or $\gamma_L\gamma_L$) $\rightarrow \pm \frac{3}{2}$ helicity $B\bar{B}'$ is a superb, direct test of the validity of the applicability of perturbative QCD to $\gamma\gamma \rightarrow B\bar{B}'$. Assuming these amplitudes are found to be zero, any discrepancy between experiments on the other helicities and the predictions of tables 3 and 4 should be small and should be attributable to an imperfect choice of the x, y, z and/or flavor-spin dependence of the wave functions, or higher-order perturbative corrections.

3. $\gamma\gamma \rightarrow p\bar{p}$ and $\gamma\gamma \rightarrow n\bar{n}$ with the Cernyak-Zhitnitsky wave function

Calculating the proton and neutron form factors, G_M^p and G_M^n , under the set of assumptions listed above for wave functions and α_s behavior, one finds [16] that neither the experimentally observed signs nor correct relative magnitudes are obtained for any of the above choices. This clearly demonstrates the inadequacy of these wave functions, or else the inadequacy of the perturbative QCD Born approximation for the nucleon form factors. Since the proton form factor has the power-law falloff $(Q^2)^{-2}$ predicted by perturbative QCD [17] for $Q^2 > 5 \text{ GeV}^2$ it is natural to suspect that the problem in these calculations of the values of the form factors is the ansätze used for the flavor-spin and/or x, y, z dependence of the nucleon wave functions. This is particularly likely since both the proton and neutron form factors come out wrong: if the asymptotic wave function and fixed α_s is used, G_M^p is zero, hence one-loop corrections to the Born approximation should be kept. Under the same conditions G_M^n is not zero, so that one-loop corrections are relatively less important. However the results for both G_M^p and G_M^n are bad, having the opposite signs to those observed experimentally. This suggests that the form of the wave function is more likely to be the culprit than the use of the Born approximation. Recently Cernyak and Zhitnitsky [13] have proposed a nucleon wave function derived from QCD sum rules. It is qualitatively different from the forms

TABLE 3

Independent amplitudes for (a) $\gamma_R \gamma_L \rightarrow B\bar{B}'$, and (b) $\gamma_R \gamma_L \rightarrow B\bar{B}'$ for the wave functions and α_s behaviors considered in table 2 (these numbers are to be multiplied by $(4\pi)^3 \alpha_{e.m.}$)

(a)		A_0	A_1	A_2	A_3
$\cos \theta$			Amplitude/ $(4\pi)^3 \alpha_{e.m.}$		
$\alpha_s = 0.2, \psi \sim (xyz)$					
0.7	-0.85E - 01	-0.36E - 01	-0.14E + 00	-0.21E + 00	
0.6	-0.60E - 01	-0.22E - 01	-0.94E - 01	-0.14E + 00	
0.5	-0.43E - 01	-0.14E - 01	-0.65E - 01	-0.97E - 01	
0.4	-0.31E - 01	-0.96E - 02	-0.45E - 01	-0.68E - 01	
0.3	-0.22E - 01	-0.64E - 02	-0.30E - 01	-0.47E - 01	
0.2	-0.14E - 01	-0.40E - 02	-0.19E - 01	-0.29E - 01	
0.1	-0.67E - 02	-0.19E - 02	-0.92E - 02	-0.14E - 01	
0.0	-0.72E - 10	0.33E - 09	0.34E - 08	-0.25E - 08	
$\alpha_s = 0.2, \psi \sim (xyz)^2$					
0.7	-0.22E - 04	-0.20E - 04	-0.38E - 04	-0.51E - 04	
0.6	-0.16E - 04	-0.13E - 04	-0.26E - 04	-0.35E - 04	
0.5	-0.11E - 04	-0.93E - 05	-0.18E - 04	-0.25E - 04	
0.4	-0.83E - 05	-0.65E - 05	-0.13E - 04	-0.18E - 04	
0.3	-0.58E - 05	-0.44E - 05	-0.88E - 05	-0.12E - 04	
0.2	-0.37E - 05	-0.27E - 05	-0.55E - 05	-0.78E - 05	
0.1	-0.18E - 05	-0.13E - 05	-0.27E - 05	-0.38E - 05	
0.0	-0.20E - 13	0.11E - 12	0.97E - 12	-0.67E - 12	
$\alpha_s = 0.2, \text{ equipartition}$					
0.7	-0.24E + 03	-0.36E + 03	-0.41E + 03	-0.47E + 03	
0.6	-0.17E + 03	-0.26E + 03	-0.30E + 03	-0.34E + 03	
0.5	-0.13E + 03	-0.19E + 03	-0.22E + 03	-0.25E + 03	
0.4	-0.92E + 02	-0.14E + 03	-0.16E + 03	-0.18E + 03	
0.3	-0.65E + 02	-0.97E + 02	-0.11E + 03	-0.13E + 03	
0.2	-0.41E + 02	-0.62E + 02	-0.72E + 02	-0.82E + 02	
0.1	-0.20E + 02	-0.30E + 02	-0.35E + 02	-0.40E + 02	
0.0	-0.74E - 16	0.12E - 14	0.84E - 14	-0.18E - 14	
$\alpha_s = \alpha_s(k^2), c1 = 1.6E - 3, c2 = 1, \psi \sim (xyz)$					
0.7	-0.31E + 00	-0.27E - 01	-0.35E + 00	-0.74E + 00	
0.6	-0.22E + 00	-0.15E - 01	-0.22E + 00	-0.48E + 00	
0.5	-0.15E + 00	-0.96E - 02	-0.15E + 00	-0.33E + 00	
0.4	-0.11E + 00	-0.62E - 02	-0.10E + 00	-0.23E + 00	
0.3	-0.76E - 01	-0.41E - 02	-0.70E - 01	-0.16E + 00	
0.2	-0.48E - 01	-0.25E - 02	-0.44E - 01	-0.99E - 01	
0.1	-0.23E - 01	-0.11E - 02	-0.21E - 01	-0.48E - 01	
0.0	-0.30E - 09	0.92E - 09	0.68E - 08	-0.75E - 08	
$\alpha_s = \alpha_s(k^2), c1 = 6.4E - 3, c2 = 1, \psi \sim (xyz)$					
0.7	-0.69E + 00	-0.27E - 01	-0.67E + 00	-0.17E + 01	
0.6	-0.48E + 00	-0.13E - 01	-0.42E + 00	-0.11E + 01	
0.5	-0.34E + 00	-0.70E - 02	-0.29E + 00	-0.76E + 00	

TABLE 3 (continued)

(a)—continued

$\cos \theta$	A_0	A_1 Amplitude/ $(4\pi)^3 \alpha_{\text{c.m.}}$	A_2	A_3
0.4	-0.24E + 00	-0.36E - 02	-0.20E + 00	-0.53E + 00
0.3	-0.17E + 00	-0.29E - 02	-0.13E + 00	-0.36E + 00
0.2	-0.11E + 00	-0.18E - 02	-0.82E - 01	-0.23E + 00
0.1	-0.52E - 01	-0.77E - 03	-0.39E - 01	-0.11E + 00
0.0	-0.89E - 09	0.14E - 08	0.14E - 07	-0.17E - 07
$\alpha_s = \alpha_s(k^2), c1 = 1.6E - 3, c2 = 1, \psi \sim (xyz)^2$				
0.7	-0.48E - 04	-0.26E - 04	-0.64E - 04	-0.11E - 03
0.6	-0.33E - 04	-0.17E - 04	-0.43E - 04	-0.74E - 04
0.5	-0.24E - 04	-0.11E - 04	-0.29E - 04	-0.52E - 04
0.4	-0.17E - 04	-0.78E - 05	-0.21E - 04	-0.37E - 04
0.3	-0.12E - 04	-0.53E - 05	-0.14E - 04	-0.26E - 04
0.2	-0.77E - 05	-0.33E - 05	-0.88E - 05	-0.16E - 04
0.1	-0.38E - 05	-0.16E - 05	-0.42E - 05	-0.78E - 05
0.0	-0.41E - 13	0.14E - 12	0.14E - 11	-0.14E - 11
$\alpha_s = \alpha_s(k^2), c1 = 6.4E - 3, c2 = 1, \psi \sim (xyz)^2$				
0.7	-0.12E - 03	-0.53E - 04	-0.15E - 03	-0.29E - 03
0.6	-0.87E - 04	-0.34E - 04	-0.95E - 04	-0.19E - 03
0.5	-0.63E - 04	-0.23E - 04	-0.66E - 04	-0.14E - 03
0.4	-0.45E - 04	-0.16E - 04	-0.46E - 04	-0.97E - 04
0.3	-0.32E - 04	-0.10E - 04	-0.31E - 04	-0.67E - 04
0.2	-0.20E - 04	-0.65E - 05	-0.19E - 04	-0.42E - 04
0.1	-0.97E - 05	-0.31E - 05	-0.93E - 05	-0.20E - 04
0.0	-0.10E - 12	0.36E - 12	0.30E - 11	-0.35E - 11
$\alpha_s = \alpha_s(k^2), c1 = 1.6E - 3, c2 = 1, \text{ equipartition}$				
0.7	-0.34E + 03	-0.42E + 03	-0.51E + 03	-0.68E + 03
0.6	-0.25E + 03	-0.31E + 03	-0.37E + 03	-0.49E + 03
0.5	-0.18E + 03	-0.23E + 03	-0.27E + 03	-0.36E + 03
0.4	-0.13E + 03	-0.16E + 03	-0.20E + 03	-0.26E + 03
0.3	-0.93E + 02	-0.12E + 03	-0.14E + 03	-0.19E + 03
0.2	-0.59E + 02	-0.74E + 02	-0.88E + 02	-0.12E + 03
0.1	-0.29E + 02	-0.36E + 02	-0.43E + 02	-0.58E + 02
0.0	0.74E - 16	0.12E - 14	0.18E - 14	-0.41E - 14
$\alpha_s = \alpha_s(k^2), c1 = 6.4E - 3, c2 = 1, \text{ equipartition}$				
0.7	-0.73E + 03	-0.83E + 03	-0.10E + 04	-0.15E + 04
0.6	-0.53E + 03	-0.60E + 03	-0.72E + 03	-0.11E + 04
0.5	-0.39E + 03	-0.44E + 03	-0.53E + 03	-0.77E + 03
0.4	-0.28E + 03	-0.32E + 03	-0.39E + 03	-0.56E + 03
0.3	-0.20E + 03	-0.23E + 03	-0.27E + 03	-0.40E + 03
0.2	-0.13E + 03	-0.14E + 03	-0.17E + 03	-0.25E + 03
0.1	-0.61E + 02	-0.70E + 02	-0.85E + 02	-0.12E + 03
0.0	0.00E + 00	0.12E - 14	0.65E - 14	-0.95E - 14

TABLE 3 (continued)

(b)

$\cos \theta$	A_0	A_1	A_2 Amplitude/ $(4\pi)^3 \alpha_{\text{e.m.}}$	A_3	A_4	A_5
$\alpha_s = 0.2, \psi \sim (xyz)$						
0.7	-0.60E - 2	-0.36E - 1	0.57E - 1	0.21E + 0	0.85E - 1	0.23E + 0
0.6	-0.11E - 1	-0.34E - 1	0.30E - 1	0.13E + 0	0.96E - 1	0.21E + 0
0.5	-0.15E - 1	-0.34E - 1	0.15E - 1	0.82E - 1	0.11E + 0	0.20E + 0
0.4	-0.19E - 1	-0.37E - 1	0.49E - 2	0.50E - 1	0.11E + 0	0.19E + 0
0.3	-0.26E - 1	-0.41E - 1	-0.27E - 2	0.27E - 1	0.12E + 0	0.19E + 0
0.2	-0.33E - 1	-0.46E - 1	-0.91E - 2	0.94E - 2	0.13E + 0	0.18E + 0
0.1	-0.42E - 1	-0.52E - 1	-0.15E - 1	-0.60E - 2	0.14E + 0	0.18E + 0
0.0	-0.51E - 1	-0.59E - 1	-0.21E - 1	-0.19E - 1	0.14E + 0	0.18E + 0
-0.1	-0.63E - 1	-0.68E - 1	-0.27E - 1	-0.31E - 1	0.15E + 0	0.18E + 0
-0.2	-0.77E - 1	-0.79E - 1	-0.35E - 1	-0.43E - 1	0.16E + 0	0.18E + 0
-0.3	-0.96E - 1	-0.94E - 1	-0.43E - 1	-0.57E - 1	0.16E + 0	0.18E + 0
-0.4	-0.12E + 0	-0.11E + 0	-0.56E - 1	-0.73E - 1	0.17E + 0	0.18E + 0
-0.5	-0.15E + 0	-0.14E + 0	-0.74E - 1	-0.93E - 1	0.18E + 0	0.19E + 0
-0.6	-0.19E + 0	-0.18E + 0	-0.10E + 0	-0.12E + 0	0.18E + 0	0.20E + 0
-0.7	-0.27E + 0	-0.25E + 0	-0.15E + 0	-0.17E + 0	0.19E + 0	0.21E + 0
$\alpha_s = 0.2, \psi \sim (xyz)^2$						
0.7	0.26E - 5	-0.45E - 5	0.14E - 4	0.52E - 4	0.20E - 4	0.43E - 4
0.6	0.72E - 6	-0.65E - 5	0.76E - 5	0.32E - 4	0.24E - 4	0.43E - 4
0.5	-0.10E - 5	-0.81E - 5	0.43E - 5	0.20E - 4	0.26E - 4	0.43E - 4
0.4	-0.28E - 5	-0.97E - 5	0.20E - 5	0.12E - 4	0.29E - 4	0.44E - 4
0.3	-0.47E - 5	-0.11E - 4	0.43E - 6	0.60E - 5	0.31E - 4	0.44E - 4
0.2	-0.68E - 5	-0.13E - 4	-0.91E - 6	0.13E - 5	0.33E - 4	0.45E - 4
0.1	-0.92E - 5	-0.15E - 4	-0.21E - 5	-0.26E - 5	0.35E - 4	0.45E - 4
0.0	-0.12E - 4	-0.18E - 4	-0.33E - 5	-0.60E - 5	0.37E - 4	0.46E - 4
-0.1	-0.15E - 4	-0.21E - 4	-0.46E - 5	-0.93E - 5	0.39E - 4	0.47E - 4
-0.2	-0.19E - 4	-0.24E - 4	-0.62E - 5	-0.13E - 4	0.41E - 4	0.48E - 4
-0.3	-0.24E - 4	-0.29E - 4	-0.82E - 5	-0.16E - 4	0.42E - 4	0.49E - 4
-0.4	-0.31E - 4	-0.35E - 4	-0.11E - 4	-0.20E - 4	0.44E - 4	0.50E - 4
-0.5	-0.40E - 4	-0.43E - 4	-0.15E - 4	-0.25E - 4	0.46E - 4	0.52E - 4
-0.6	-0.52E - 4	-0.55E - 4	-0.22E - 4	-0.32E - 4	0.47E - 4	0.54E - 4
-0.7	-0.71E - 4	-0.75E - 4	-0.33E - 4	-0.44E - 4	0.48E - 4	0.56E - 4
$\alpha_s = 0.2, \text{ equipartition}$						
0.7	0.32E + 2	0.61E + 2	0.13E + 3	0.49E + 3	0.19E + 3	0.23E + 3
0.6	0.12E + 2	0.13E + 2	0.88E + 2	0.31E + 3	0.22E + 3	0.27E + 3
0.5	-0.58E + 1	-0.23E + 2	0.62E + 2	0.20E + 3	0.25E + 3	0.31E + 3
0.4	-0.24E + 2	-0.54E + 2	0.45E + 2	0.12E + 3	0.28E + 3	0.34E + 3
0.3	-0.43E + 2	-0.83E + 2	0.33E + 2	0.54E + 2	0.30E + 3	0.38E + 3
0.2	-0.65E + 2	-0.11E + 3	0.25E + 2	0.47E + 1	0.33E + 3	0.41E + 3
0.1	-0.90E + 2	-0.14E + 3	0.18E + 2	-0.37E + 2	0.35E + 3	0.44E + 3
0.0	-0.12E + 3	-0.18E + 3	0.10E + 2	-0.73E + 2	0.37E + 3	0.47E + 3
-0.1	-0.15E + 3	-0.22E + 3	0.12E + 1	-0.11E + 3	0.40E + 3	0.49E + 3
-0.2	-0.20E + 3	-0.26E + 3	-0.11E + 2	-0.14E + 3	0.42E + 3	0.52E + 3
-0.3	-0.25E + 3	-0.32E + 3	-0.29E + 2	-0.17E + 3	0.43E + 3	0.54E + 3
-0.4	-0.32E + 3	-0.40E + 3	-0.55E + 2	-0.21E + 3	0.45E + 3	0.56E + 3
-0.5	-0.42E + 3	-0.51E + 3	-0.94E + 2	-0.25E + 3	0.46E + 3	0.58E + 3
-0.6	-0.56E + 3	-0.65E + 3	-0.16E + 3	-0.31E + 3	0.47E + 3	0.58E + 3

TABLE 3 (continued)

(b)—continued

$\cos \theta$	A_0	A_1	A_2	A_3	A_4	A_5
	Amplitude/ $(4\pi)^3 \alpha_{\text{se.m.}}$					
$\alpha_s = \alpha(k^2), c1 = 1.6E - 3, c2 = 1, \psi \sim (xyz)$						
0.7	-0.39E - 1	-0.17E + 0	0.24E + 0	0.41E + 0	0.26E + 0	0.59E + 0
0.6	-0.38E - 1	-0.13E + 0	0.14E + 0	0.21E + 0	0.29E + 0	0.52E + 0
0.5	-0.73E - 1	-0.11E + 0	0.84E - 1	0.97E - 1	0.32E + 0	0.48E + 0
0.4	-0.77E - 1	-0.11E + 0	0.48E - 1	0.14E - 1	0.35E + 0	0.45E + 0
0.3	-0.84E - 1	-0.11E + 0	0.22E - 1	-0.44E - 1	0.37E + 0	0.42E + 0
0.2	-0.90E - 1	-0.12E + 0	-0.35E - 2	-0.93E - 1	0.40E + 0	0.42E + 0
0.1	-0.13E + 0	-0.13E + 0	-0.23E - 1	-0.13E + 0	0.42E + 0	0.41E + 0
0.0	-0.16E + 0	-0.14E + 0	-0.42E - 1	-0.17E + 0	0.44E + 0	0.41E + 0
-0.1	-0.19E + 0	-0.16E + 0	-0.64E - 1	-0.21E + 0	0.46E + 0	0.39E + 0
-0.2	-0.24E + 0	-0.18E + 0	-0.86E - 1	-0.26E + 0	0.49E + 0	0.40E + 0
-0.3	-0.28E + 0	-0.20E + 0	-0.11E + 0	-0.31E + 0	0.52E + 0	0.40E + 0
-0.4	-0.33E + 0	-0.24E + 0	-0.15E + 0	-0.38E + 0	0.54E + 0	0.41E + 0
-0.5	-0.42E + 0	-0.29E + 0	-0.21E + 0	-0.47E + 0	0.58E + 0	0.43E + 0
-0.6	-0.57E + 0	-0.36E + 0	-0.30E + 0	-0.62E + 0	0.61E + 0	0.45E + 0
-0.7	-0.76E + 0	-0.50E + 0	-0.45E + 0	-0.87E + 0	0.66E + 0	0.48E + 0
$\alpha_s = \alpha_s(k^2), c1 = 6.4E - 3, c2 = 1, \psi \sim (xyz)$						
0.7	-0.56E - 2	-0.43E + 0	0.45E + 0	0.91E + 0	0.56E + 0	0.13E + 1
0.6	-0.29E - 1	-0.34E + 0	0.26E + 0	0.47E + 0	0.64E + 0	0.11E + 1
0.5	-0.64E - 1	-0.29E + 0	0.14E + 0	0.20E + 0	0.70E + 0	0.98E + 0
0.4	-0.99E - 1	-0.27E + 0	0.79E - 1	0.20E - 1	0.76E + 0	0.92E + 0
0.3	-0.14E + 0	-0.27E + 0	0.25E - 1	-0.11E + 0	0.82E + 0	0.86E + 0
0.2	-0.18E + 0	-0.27E + 0	-0.19E - 1	-0.21E + 0	0.87E + 0	0.83E + 0
0.1	-0.23E + 0	-0.29E + 0	-0.57E - 1	-0.30E + 0	0.92E + 0	0.80E + 0
0.0	-0.29E + 0	-0.31E + 0	-0.92E - 1	-0.39E + 0	0.98E + 0	0.80E + 0
-0.1	-0.36E + 0	-0.34E + 0	-0.13E + 0	-0.48E + 0	0.10E + 1	0.79E + 0
-0.2	-0.44E + 0	-0.38E + 0	-0.18E + 0	-0.58E + 0	0.11E + 1	0.79E + 0
-0.3	-0.55E + 0	-0.44E + 0	-0.23E + 0	-0.69E + 0	0.11E + 1	0.81E + 0
-0.4	-0.68E + 0	-0.51E + 0	-0.30E + 0	-0.85E + 0	0.12E + 1	0.83E + 0
-0.5	-0.88E + 0	-0.62E + 0	-0.41E + 0	-0.11E + 1	0.13E + 1	0.86E + 0
-0.6	-0.12E + 1	-0.78E + 0	-0.58E + 0	-0.14E + 1	0.13E + 1	0.90E + 0
-0.7	-0.16E + 1	-0.11E + 1	-0.89E + 0	-0.19E + 1	0.14E + 1	0.98E + 0
$\alpha_s = \alpha_s(k^2), c1 = 1.6E - 3, c2 = 1, \psi \sim (xyz)^2$						
0.7	0.12E - 4	-0.19E - 4	0.32E - 4	0.83E - 4	0.40E - 4	0.73E - 4
0.6	0.73E - 5	-0.19E - 4	0.19E - 4	0.48E - 4	0.46E - 4	0.71E - 4
0.5	0.32E - 5	-0.20E - 4	0.12E - 4	0.26E - 4	0.51E - 4	0.70E - 4
0.4	-0.77E - 6	-0.22E - 4	0.72E - 5	0.12E - 4	0.56E - 4	0.70E - 4
0.3	-0.49E - 5	-0.23E - 4	0.36E - 5	0.93E - 6	0.60E - 4	0.70E - 4
0.2	-0.92E - 5	-0.26E - 4	0.66E - 6	-0.75E - 5	0.65E - 4	0.70E - 4
0.1	-0.14E - 4	-0.28E - 4	-0.20E - 5	-0.15E - 4	0.69E - 4	0.71E - 4
0.0	-0.19E - 4	-0.32E - 4	-0.46E - 5	-0.22E - 4	0.73E - 4	0.71E - 4
-0.1	-0.26E - 4	-0.36E - 4	-0.73E - 5	-0.28E - 4	0.77E - 4	0.73E - 4
-0.2	-0.33E - 4	-0.41E - 4	-0.10E - 4	-0.35E - 4	0.81E - 4	0.74E - 4
-0.3	-0.43E - 4	-0.48E - 4	-0.15E - 4	-0.43E - 4	0.85E - 4	0.76E - 4
-0.4	-0.55E - 4	-0.57E - 4	-0.20E - 4	-0.52E - 4	0.89E - 4	0.79E - 4
-0.5	-0.71E - 4	-0.70E - 4	-0.28E - 4	-0.65E - 4	0.93E - 4	0.82E - 4
-0.6	-0.95E - 4	-0.89E - 4	-0.40E - 4	-0.82E - 4	0.87E - 4	0.82E - 4

TABLE 3 (continued)

(b)—continued

$\cos \theta$	A_0	A_1	A_2	A_3	A_4	A_5
	Amplitude/ $(4\pi)^3 \alpha_{e.m.}$					
$\alpha_s = \alpha_s(K^2)$, $c1 = 6.4E - 3$, $c2 = 1$, $\psi \sim (xyz)^2$						
0.7	0.47E - 4	-0.55E - 4	0.81E - 4	0.19E - 3	0.10E - 3	0.17E - 3
0.6	0.33E - 4	-0.52E - 4	0.49E - 4	0.11E - 3	0.12E - 3	0.16E - 3
0.5	0.21E - 4	-0.52E - 4	0.31E - 4	0.54E - 4	0.13E - 3	0.16E - 3
0.4	0.10E - 4	-0.54E - 4	0.19E - 4	0.18E - 4	0.14E - 3	0.16E - 3
0.3	-0.96E - 6	-0.57E - 4	0.10E - 4	-0.80E - 5	0.15E - 3	0.16E - 3
0.2	-0.13E - 4	-0.61E - 4	0.31E - 5	-0.29E - 4	0.16E - 3	0.15E - 3
0.1	-0.25E - 4	-0.67E - 4	-0.34E - 5	-0.47E - 4	0.17E - 3	0.16E - 3
0.0	-0.39E - 4	-0.74E - 4	-0.95E - 5	-0.64E - 4	0.19E - 3	0.16E - 3
-0.1	-0.55E - 4	-0.84E - 4	-0.16E - 4	-0.81E - 4	0.20E - 3	0.16E - 3
-0.2	-0.74E - 4	-0.95E - 4	-0.23E - 4	-0.99E - 4	0.21E - 3	0.16E - 3
-0.3	-0.98E - 4	-0.11E - 3	-0.33E - 4	-0.12E - 3	0.22E - 3	0.17E - 3
-0.4	-0.13E - 3	-0.13E - 3	-0.46E - 4	-0.15E - 3	0.23E - 3	0.17E - 3
-0.5	-0.17E - 3	-0.16E - 3	-0.64E - 4	-0.18E - 3	0.24E - 3	0.18E - 3
-0.6	-0.22E - 3	-0.20E - 3	-0.92E - 4	-0.23E - 3	0.25E - 3	0.19E - 3
-0.7	-0.31E - 3	-0.27E - 3	-0.14E - 3	-0.31E - 3	0.26E - 3	0.20E - 3
$\alpha_s = \alpha_s(k^2)$, $c1 = 1.6E - 3$, $c2 = 1$, equipartition						
0.7	0.80E + 2	0.54E + 2	0.18E + 3	0.70E + 3	0.27E + 3	0.28E + 3
0.6	0.52E + 2	-0.89E + 0	0.12E + 3	0.45E + 3	0.32E + 3	0.33E + 3
0.5	0.26E + 2	-0.43E + 2	0.86E + 2	0.29E + 3	0.36E + 3	0.38E + 3
0.4	0.11E + 1	-0.80E + 2	0.63E + 2	0.17E + 3	0.40E + 3	0.42E + 3
0.3	-0.25E + 2	-0.11E + 3	0.47E + 2	0.78E + 2	0.43E + 3	0.46E + 3
0.2	-0.55E + 2	-0.15E + 3	0.35E + 2	0.67E + 1	0.47E + 3	0.50E + 3
0.1	-0.89E + 2	-0.19E + 3	0.25E + 2	-0.52E + 2	0.50E + 3	0.53E + 3
0.0	-0.13E + 3	-0.23E + 3	0.15E + 2	-0.10E + 3	0.54E + 3	0.57E + 3
-0.1	-0.18E + 3	-0.28E + 3	0.24E + 1	-0.15E + 3	0.57E + 3	0.60E + 3
-0.2	-0.24E + 3	-0.34E + 3	-0.14E + 2	-0.20E + 3	0.60E + 3	0.63E + 3
-0.3	-0.31E + 3	-0.42E + 3	-0.36E + 2	-0.25E + 3	0.62E + 3	0.66E + 3
-0.4	-0.41E + 3	-0.52E + 3	-0.69E + 2	-0.30E + 3	0.65E + 3	0.68E + 3
-0.5	-0.54E + 3	-0.65E + 3	-0.12E + 3	-0.36E + 3	0.66E + 3	0.70E + 3
-0.6	-0.73E + 3	-0.84E + 3	-0.19E + 3	-0.45E + 3	0.67E + 3	0.71E + 3
-0.7	-0.10E + 4	-0.11E + 4	-0.31E + 3	-0.56E + 3	0.66E + 3	0.70E + 3
$\alpha_s = \alpha_s(k^2)$, $c1 = 6.4E - 3$, $c2 = 1$, equipartition						
0.7	0.20E + 3	0.88E + 2	0.38E + 3	0.15E + 4	0.57E + 3	0.56E + 3
0.6	0.14E + 3	-0.17E + 2	0.25E + 3	0.96E + 3	0.67E + 3	0.65E + 3
0.5	0.84E + 2	-0.99E + 2	0.18E + 3	0.61E + 3	0.76E + 3	0.74E + 3
0.4	0.31E + 2	-0.17E + 3	0.13E + 3	0.36E + 3	0.84E + 3	0.82E + 3
0.3	-0.25E + 2	-0.24E + 3	0.98E + 2	0.17E + 3	0.92E + 3	0.90E + 3
0.2	-0.87E + 2	-0.31E + 3	0.73E + 2	0.14E + 2	0.10E + 4	0.97E + 3
0.1	-0.16E + 3	-0.39E + 3	0.52E + 2	-0.11E + 3	0.11E + 4	0.10E + 4
0.0	-0.24E + 3	-0.47E + 3	0.31E + 2	-0.22E + 3	0.11E + 4	0.11E + 4
-0.1	-0.34E + 3	-0.57E + 3	0.55E + 1	-0.32E + 3	0.12E + 4	0.12E + 4
-0.2	-0.46E + 3	-0.69E + 3	-0.27E + 2	-0.42E + 3	0.13E + 4	0.12E + 4
-0.3	-0.62E + 3	-0.85E + 3	-0.72E + 2	-0.52E + 3	0.13E + 4	0.13E + 4
-0.4	-0.83E + 3	-0.10E + 4	-0.14E + 3	-0.64E + 3	0.14E + 4	0.13E + 4
-0.5	-0.11E + 4	-0.13E + 4	-0.23E + 3	-0.77E + 3	0.14E + 4	0.14E + 4
-0.6	-0.15E + 4	-0.17E + 4	-0.38E + 3	-0.95E + 3	0.14E + 4	0.14E + 4

TABLE 4

$\gamma\gamma \rightarrow p\bar{p}$ unpolarized cross section $s^6 d\sigma/dt$ in nb · GeV¹⁰ for the various choices of wave functions and α_s behavior considered in table 1: $(xyz)^1$, $(xyz)^2$, and equipartition

$\cos \theta$	$(xyz)^1$	$(xyz)^2$	Equipartition
$\alpha = 0.183$			
0.7	0.19E + 04	0.19E + 04	0.21E + 04
0.6	0.99E + 03	0.10E + 04	0.11E + 04
0.5	0.58E + 03	0.60E + 03	0.67E + 03
0.4	0.36E + 03	0.37E + 03	0.41E + 03
0.3	0.24E + 03	0.24E + 03	0.26E + 03
0.2	0.17E + 03	0.16E + 03	0.17E + 03
0.1	0.13E + 03	0.12E + 03	0.13E + 03
0.0	0.12E + 03	0.11E + 03	0.11E + 03
$\alpha = \alpha(k^2)$, c1 = 1.6E - 3, c2 = 1			
0.7	0.43E + 04	0.30E + 04	0.24E + 04
0.6	0.23E + 04	0.16E + 04	0.13E + 04
0.5	0.13E + 04	0.90E + 03	0.75E + 03
0.4	0.83E + 03	0.55E + 03	0.44E + 03
0.3	0.59E + 03	0.35E + 03	0.27E + 03
0.2	0.44E + 03	0.23E + 03	0.17E + 03
0.1	0.37E + 03	0.18E + 03	0.12E + 03
0.0	0.34E + 03	0.16E + 03	0.10E + 03
$\alpha = \alpha(k^2)$, c1 = 6.4E - 3, c2 = 1			
0.7	0.59E + 04	0.47E + 04	0.34E + 04
0.6	0.31E + 04	0.24E + 04	0.18E + 04
0.5	0.18E + 04	0.14E + 04	0.10E + 04
0.4	0.11E + 04	0.83E + 03	0.60E + 03
0.3	0.74E + 03	0.51E + 03	0.36E + 03
0.2	0.52E + 03	0.33E + 03	0.22E + 03
0.1	0.42E + 03	0.24E + 03	0.14E + 03
0.0	0.39E + 03	0.21E + 03	0.12E + 03

used above because it is not symmetric in x, y, z and does not have the asymptotic SU(6) dependence on flavor and spin. Using it with fixed $\alpha_s = 0.3$ they find relatively good agreement with $\psi \rightarrow p\bar{p}$ and G_M^p and G_M^n : factor-of-two agreement on all the magnitudes of the amplitudes, the correct signs for G_M^p and G_M^n , and agreement on the ratio G_M^p/G_M^n ($\approx -\frac{1}{2}$) to within experimental errors. This is particularly impressive considering that they predict the absolute normalization as well as the form of their wave function.

A priori, it is not evident whether other processes than the nucleon form factor will be so sensitive to the x, y, z and flavor-spin dependence of the nucleon wave function, and it is necessary to carry out the calculations of the cross sections for $\gamma\gamma \rightarrow p\bar{p}$ and $\gamma\gamma \rightarrow n\bar{n}$ with the CZ wave function to find out. (Because the CZ wave

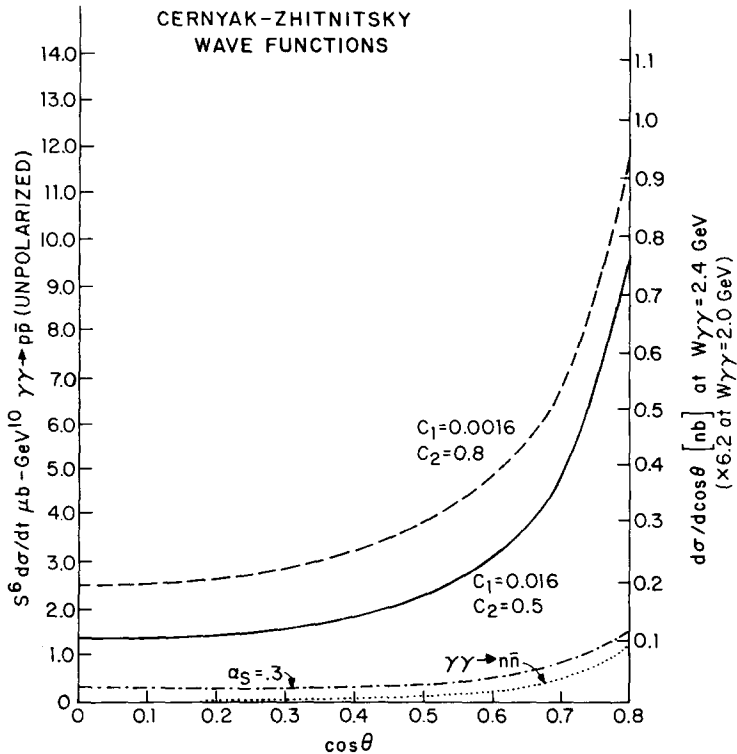


Fig. 2. $s^6 \frac{d\sigma}{dt}$ in $\mu b \cdot GeV^{10}$ for $\gamma\gamma \rightarrow p\bar{p}$ using CZ wave functions with $c_1 = 0.016$, $c_2 = 0.5$ (solid line), $c_1 = 0.0016$, $c_2 = 0.8$ (dashed line), and $\alpha_s = 0.3$ (dot-dashed line), and for $\gamma\gamma \rightarrow n\bar{n}$ with $c_1 = 0.016$, $c_2 = 0.5$ (dotted line).

function does not have the simple SU(6) asymptotic flavor-spin dependence, it is not possible using the results of their paper to compute the amplitudes for the other reactions such as $\gamma\gamma \rightarrow \Delta^{++} \bar{\Delta}^{++}$. The results for fixed $\alpha_s = 0.3$ and for running α_s with two choices of c_1 and c_2 are reproduced from [16] in fig. 2. The choice $c_1 = 0.016$, $c_2 = 0.5$ is the most attractive, corresponding to $\Lambda = 0.2$ GeV at $s = 10$ GeV² with α_s restricted to be more plausibly in the perturbative regime than for larger values of c_2 ($\equiv \alpha_s^{\max}$); happily these values ($c_1 = 0.016$, $c_2 = 0.5$) give [16] very good agreement with experiment for $\psi \rightarrow p\bar{p}$, G_M^p and G_M^n – even better than the fixed $\alpha_s = 0.3$ used by Cernyak and Zhitnitsky in their calculations, presumably for simplicity. The solid curve in fig. 2, corresponding to $c_1 = 0.016$, $c_2 = 0.5$, should probably therefore be regarded as the “best” prediction for $\gamma\gamma \rightarrow p\bar{p}$ using the CZ wave function. The fact that using running α_s and $c_2 = 0.5$ gives a prediction greater by a factor of six or more than that obtained with fixed $\alpha_s = 0.3$ indicates that with the CZ wave function, quarks carrying small-momentum fractions make an important contribution to the scattering amplitude. It is not yet possible to be certain,

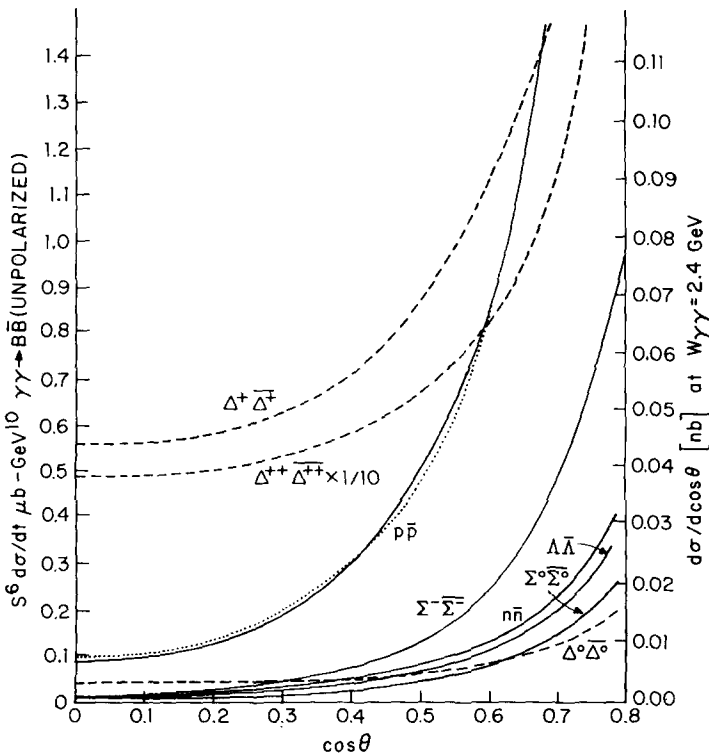


Fig. 3. $s^6 d\sigma/dt$ in $\mu b \cdot \text{GeV}^{10}$ for unpolarized $\gamma\gamma \rightarrow p\bar{p}$, $\Sigma^- \bar{\Sigma}^-$, $n\bar{n}$, $\Lambda \bar{\Lambda}$, $\Sigma^0 \bar{\Sigma}^0$, $\Delta^0 \bar{\Delta}^0$, $\Delta^+ \bar{\Delta}^+$ and (reduced by factor of 10) $\Delta^{++} \bar{\Delta}^{++}$, using the “equipartition” wave function*. The prediction using the “asymptotic” wave function is shown for $p\bar{p}$, with a dotted line. The cross section for $p\bar{\Delta}^+$ is not shown because it is equal to that for $\Sigma^0 \bar{\Sigma}^0$ within the accuracy of the figure, nor is the $\Lambda \bar{\Sigma}^0$ cross section which would be indistinguishable from zero.

on either theoretical or experimental grounds, whether the Born approximation should be adequate in this case.

4. Discussion

For orientation to the various predictions, fig. 3 shows the unpolarized cross sections summed over final helicities for all $\gamma\gamma \rightarrow B\bar{B}'$ reactions*, taking fixed $\alpha_s = 0.2$ and using the “equipartition” wave functions. For $\gamma\gamma \rightarrow p\bar{p}$ the asymptotic wave-function prediction is also shown. At least for fixed α_s this demonstrates the insensitivity of the prediction to the wave-function choice, as long as it is symmetric

* The cross sections for $Y^* \bar{Y}^*$, $\Xi^* \bar{\Xi}^*$, and $\Omega^- \bar{\Omega}^-$ production = $\frac{1}{16}$ that of $\Delta^{++} \bar{\Delta}^{++}$ (by $u \leftrightarrow d$ and $d \leftrightarrow s$), and $Y^* \bar{Y}^* \equiv \Delta^+ \bar{\Delta}^+$, and $Y^* Y^* \equiv \Xi^0 \bar{\Xi}^0 \equiv \Delta^0 \bar{\Delta}^0$.

and has the asymptotic SU(6) flavor-spin dependence. On the other hand, comparing fig. 2 and fig. 3 shows that using the CZ wave function instead of a symmetric wave function makes a very big difference in the angular behavior and magnitude of the $\gamma\gamma \rightarrow p\bar{p}$ prediction. Fig. 3 also illustrates that $\gamma\gamma \rightarrow \Delta^+ \bar{\Delta}^+$ and $\gamma\gamma \rightarrow \Delta^{++} \bar{\Delta}^{++}$ may be much larger than $\gamma\gamma \rightarrow p\bar{p}$, by factors of 6 and 50 respectively at 90° , making them feasible channels to study. Unfortunately other channels will probably be very hard to study experimentally. It is a shame that we do not have sum-rule-derived wave functions for the full octet and decuplet of final-state baryons in order to present the analog of fig. 3 for “CZ” wave functions.

The ratio $r \equiv \Gamma(\psi \rightarrow p\bar{p})/\Gamma(\psi \rightarrow e^+e^-)$ is proportional to $\alpha_s^6 \phi_B^4$. Therefore for fixed α_s the $\gamma\gamma \rightarrow B\bar{B}$ cross section, which is proportional to $\alpha_s^4 \phi_B^4$, behaves as $\alpha_s^{-2} r$. Thus when the nucleon wave function is normalized by demanding $r = 0.029$ as is experimentally observed, increasing the value taken for α_s decreases the prediction for $\gamma\gamma \rightarrow B\bar{B}$ and conversely. For instance, changing from fixed $\alpha_s = 0.2$ to $\alpha_s = 0.15$ increases the cross-section predictions of fig. 2 by a factor 1.8 while taking $\alpha_s = 0.27$ decreases them by a factor 0.54*. This factor-of-two uncertainty is fairly representative of the range of results obtained using the various models of running couplings listed in table 1, as reflected in the $\gamma\gamma \rightarrow p\bar{p}$ cross sections in table 4. The changes in the angular dependence resulting from changing the prescription for the running coupling can also be qualitatively understood. Some of the gluon propagators have k^2 's proportional to t , so that going to smaller angles with a running coupling constant typically increases the mean value of α_s relative to its mean value for 90° scattering. With running couplings on the light quark vertices in $\psi \rightarrow p\bar{p}$, r scales as the running coupling cubed so that $\sigma(\gamma\gamma \rightarrow B\bar{B}) \sim \alpha_{\text{running}}^{+1} r$. Thus a larger value for α_s increases the predicted $\gamma\gamma \rightarrow p\bar{p}$ cross sections and sharpens the angular distribution. The extent of the increase in $\langle \alpha_s \rangle$ as t decreases depends on the rate of change of α_s with $\langle k^2 \rangle$, which depends on c_1 .

Table 5 shows the predicted cross sections, $s^6 d\sigma/dt$ and integrated cross sections for $|\cos \theta| < 0.75$, for fixed $\alpha_s = 0.2$ and asymptotic and equipartition wave functions separately for $RL \rightarrow (\frac{1}{2}, -\frac{1}{2})$, $RL \rightarrow (\frac{3}{2}, -\frac{3}{2})$, and $RR \rightarrow (\frac{1}{2}, -\frac{1}{2})$ for all octet and decuplet baryons**. $RR \rightarrow (\frac{3}{2}, -\frac{3}{2})$ is not listed because it is identically zero, as discussed above. This table is included to emphasize the strong helicity dependence of the $\gamma\gamma \rightarrow B\bar{B}'$ reactions. We hope that the dramatic features which are manifest upon inspecting these predictions, combined with the fundamental importance of measuring $\gamma_R \gamma_L$ and/or $\gamma_L \gamma_L \rightarrow B_{\pm 3/2} \bar{B}'_{\mp 3/2}$ and helicity non-conserving reactions such as $\gamma\gamma \rightarrow B_{+1/2} \bar{B}'_{+1/2}$ or $B_{-1/2} \bar{B}'_{-1/2}$ will encourage development of the necessary tools for measuring these polarized cross sections.

* Damgaard uses the normalization method proposed in ref. [14] to calculate $\tilde{r} = \Gamma(\psi \rightarrow p\bar{p})/\Gamma(\psi \rightarrow 3 \text{ gluons})$. For fixed $\alpha_s = 0.2$ this method yields the same value of ϕ_p as ours does, but since $\sigma(\gamma\gamma \rightarrow p\bar{p}) \sim \alpha_s^2 r^2$ and $\sim \alpha_s^{-1} \tilde{r}^2$ the two normalization methods lead to different predictions for $\gamma\gamma \rightarrow p\bar{p}$ when smaller or larger values of α_s are taken.

** See footnote on previous page.

TABLE 5a
 $s^6 d\sigma/dt$ and $s^5 \Delta\sigma$ for $|\cos\theta| < 0.75$, for unpolarized $\gamma\gamma \rightarrow B\bar{B}'$ in nb · GeV¹⁰,
using asymptotic wave functions (in this table $\alpha_s = 0.2$)

$\cos\theta$	$p\bar{p}$	$n\bar{n}$	$\Sigma^- \bar{\Sigma}^-$	$\Lambda \bar{\Lambda}$	$\Sigma^0 \bar{\Sigma}^0$	$\Lambda \bar{\Sigma}^0$	$p \bar{\Delta}^+$	$\Lambda^{++} \bar{\Lambda}^{++}$	$\Lambda^+ \bar{\Lambda}^+$	$\Lambda^0 \bar{\Lambda}^0$
0.7	0.15E + 4	0.30E + 3	0.59E + 3	0.28E + 3	0.26E + 3	0.30E + 1	0.21E + 3	0.17E + 5	0.24E + 4	0.20E + 3
0.6	0.84E + 3	0.16E + 3	0.28E + 3	0.15E + 3	0.14E + 3	0.11E + 1	0.10E + 3	0.12E + 5	0.16E + 4	0.13E + 3
0.5	0.49E + 3	0.85E + 2	0.15E + 3	0.82E + 2	0.78E + 2	0.46	0.54E + 2	0.95E + 4	0.12E + 4	0.99E + 2
0.4	0.30E + 3	0.49E + 2	0.89E + 2	0.48E + 2	0.45E + 2	0.17	0.32E + 2	0.82E + 4	0.99E + 3	0.79E + 2
0.3	0.20E + 3	0.30E + 2	0.53E + 2	0.28E + 2	0.27E + 2	0.73E - 1	0.20E + 2	0.75E + 4	0.89E + 3	0.67E + 2
0.2	0.14E + 3	0.18E + 2	0.35E + 2	0.17E + 2	0.16E + 2	0.35E - 1	0.14E + 2	0.70E + 4	0.82E + 3	0.60E + 2
0.1	0.11E + 3	0.12E + 2	0.26E + 2	0.11E + 2	0.10E + 2	0.17E - 1	0.10E + 2	0.68E + 4	0.79E + 3	0.56E + 2
0	0.10E + 3	0.98E + 1	0.23E + 2	0.95E + 1	0.89E + 1	0.70E - 2	0.11E + 2	0.69E + 4	0.80E + 3	0.56E + 2
						Integrated cross section for $ \cos\theta < 0.75$				
	0.37E + 3	0.65E + 2	0.12E + 3	0.62E + 2	0.58E + 2	0.48	0.45E + 2	0.72E + 4	0.92E + 3	0.73E + 2

TABLE 5b
As above, using equipartition wave functions.

$\cos\theta$	$p\bar{p}$	$n\bar{n}$	$\Sigma^- \bar{\Sigma}^-$	$\Lambda \bar{\Lambda}$	$\Sigma^0 \bar{\Sigma}^0$	$\Lambda \bar{\Sigma}^0$	$p \bar{\Delta}^+$	$\Lambda^{++} \bar{\Lambda}^{++}$	$\Lambda^+ \bar{\Lambda}^+$	$\Lambda^0 \bar{\Lambda}^0$
0.9	0.90E + 4	0.12E + 4	0.31E + 4	0.11E + 4	0.82E + 3	0.33E + 2	0.79E + 3	0.52E + 5	0.76E + 4	0.54E + 3
0.8	0.33E + 4	0.47E + 3	0.11E + 4	0.41E + 3	0.31E + 3	0.10E + 2	0.30E + 3	0.21E + 5	0.30E + 4	0.22E + 3
0.7	0.16E + 4	0.24E + 3	0.48E + 3	0.21E + 3	0.15E + 3	0.48E + 1	0.15E + 3	0.12E + 5	0.17E + 4	0.13E + 3
0.6	0.86E + 3	0.14E + 3	0.25E + 3	0.12E + 3	0.83E + 2	0.26E + 1	0.91E + 2	0.86E + 4	0.12E + 4	0.94E + 2
0.5	0.51E + 3	0.85E + 2	0.14E + 3	0.71E + 2	0.50E + 2	0.16E + 1	0.56E + 2	0.69E + 4	0.89E + 3	0.70E + 2
0.4	0.31E + 3	0.54E + 2	0.76E + 2	0.45E + 2	0.30E + 2	0.12E + 1	0.38E + 2	0.60E + 4	0.74E + 3	0.56E + 2
0.3	0.20E + 3	0.36E + 2	0.43E + 2	0.30E + 2	0.19E + 2	0.89	0.27E + 2	0.54E + 4	0.66E + 3	0.49E + 2
0.2	0.13E + 3	0.25E + 2	0.23E + 2	0.20E + 2	0.12E + 2	0.76	0.21E + 2	0.51E + 4	0.60E + 3	0.43E + 2
0.1	0.97E + 2	0.19E + 2	0.13E + 2	0.15E + 2	0.84E + 1	0.71	0.18E + 2	0.50E + 4	0.58E + 3	0.41E + 2
0	0.86E + 2	0.17E + 2	0.10E + 2	0.13E + 2	0.74E + 1	0.69	0.17E + 2	0.50E + 4	0.57E + 3	0.40E + 2
						Integrated cross section for $ \cos\theta < 0.75$				
	0.37E + 3	0.60E + 2	0.10E + 3	0.51E + 2	0.36E + 2	0.13E + 1	0.41E + 2	0.51E + 4	0.66E + 3	0.51E + 2

5. Comparison with previous calculation

The unpolarized cross section for $\gamma\gamma \rightarrow p\bar{p}$ has previously been computed by Damgaard [8] for fixed $\alpha_s = 0.27$ and three wave function choices: equipartition, $(xyz)^{3/2}\delta(1-x-y-z)$, and $(xyz)^2\delta(1-x-y-z)$. Our results should be identical with his when the same wave function and coupling constants are taken. However we find an angular dependence which is significantly flatter than his and our prediction for the magnitude is much smaller, by a factor of 20–100 depending on how ϕ_B is normalized. Damgaard's calculation differs from ours in that he calculated a subset of diagrams (actually, for the Compton scattering kinematics $\gamma p \rightarrow \gamma p$) in Feynman gauge and used symmetries to generate the full set of diagrams from them, finally crossing the full amplitude to the annihilation channel. Although in principle this is a workable approach, in practice it has the drawback of requiring absolute accuracy in calculation and absolute accuracy in sorting out relative phases between diagrams related by various symmetries. A virtue of calculating all diagrams

in an arbitrary gauge, as we do, is that (in addition to not being reliant on making correct use of symmetries between diagrams) we have at our disposal some very powerful tests of the validity of the result. We know that it is independent of SU(3) and U(1) gauge parameters, a highly non-trivial check of a sum of ~ 50 diagrams. Furthermore we can calculate amplitudes which are in principle redundant on account of charge conjugation, parity invariance, and Bose symmetry of two same-helicity photons, as discussed above, and verify that our amplitudes have the required symmetry properties. In view of the discrepancy between our result and Damgaard's we have explicitly checked all relations of this kind. As a result of the checks mentioned above and in the introduction we are confident of the correctness of our calculations.

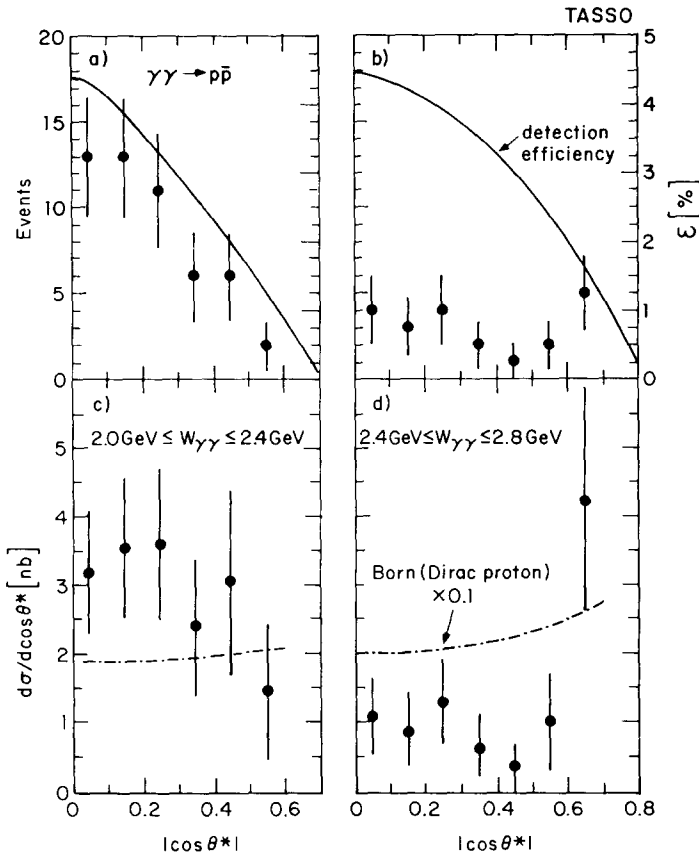
6. Comparison with experiment

How do these predictions compare with experiment? The $\gamma\gamma \rightarrow p\bar{p}$ cross section has been measured [2] out to 90° for $W_{\gamma\gamma} < 2.8$ GeV ($t \lesssim 3$ GeV 2) with the bulk of the events in the $W_{\gamma\gamma} = 2.0\text{--}2.4$ GeV range. $d\sigma/d\cos\theta$ is measured to be virtually constant (see fig. 4). In the $2.0 < W_{\gamma\gamma} < 2.4$ GeV bin it is $\sim 3 \pm 1$ nb, and in the $2.4 < W_{\gamma\gamma} < 2.8$ GeV bin it is $\sim 1 \pm 0.5$ nb.

Since the onset of the asymptotic (Q^2) falloff of G_M^p only occurs at $t \gtrsim 5$ GeV 2 , this data may be at too low a t value to be accurately predicted by the lowest-twist Born approximation perturbative QCD calculation. Moreover there are known resonances such as the states at 2190 and 2350 MeV which have been seen in $p\bar{p}$ elastic [18] and total [19] cross sections, and in $p\bar{p} \rightarrow n\bar{n}$ [20], which could contribute to $\gamma\gamma \rightarrow p\bar{p}$ in this relatively low $W_{\gamma\gamma}$ range and possibly swamp the perturbative QCD contribution. On the other hand perturbative QCD has often surprised us by its precocity. For instance, the perturbative QCD prediction for $\gamma\gamma \rightarrow \pi^+\pi^-$ [11] is apparently in reasonable agreement with the data for the $W_{\gamma\gamma}$ range 1.6–2.8 GeV [1]. Therefore it is interesting to compare the results of these calculations to the existing $\gamma\gamma \rightarrow p\bar{p}$ data.

The right vertical axis in figs. 2 and 3 gives the values of $d\sigma/d\cos\theta$ in nb for $W_{\gamma\gamma} = 2.4$ GeV. Multiplying by 6.2 gives $d\sigma/d\cos\theta$ for $W_{\gamma\gamma} = 2.0$ GeV. One sees that the predictions using the symmetric wave functions (fig. 3) are far below the experimental result of ~ 2 nb. The prediction of the CZ wave function (solid line, fig. 2) gives a much better accounting of the data, both its shape and magnitude. Integrating the solid curve CZ prediction of fig. 3 for $|\cos\theta| < 0.6$ gives ~ 0.17 nb at $W = 2.4$ GeV, ~ 1 nb at 2 GeV.

What conclusion can we draw from the present evidence? The data is above the prediction even of the CZ wave function, but with large error bars. Further theoretical study of the uncertainty in the QCD prediction, e.g., coming from uncertainty in the “CZ” wave function and α_s behavior, is clearly needed. Although the data may be consistent with Born approximation perturbative QCD even in this

Fig. 4. $\gamma\gamma \rightarrow p\bar{p}$ data from ref. [2].

rather low $W_{\gamma\gamma}$ and t regime, we cannot rule out the possibility that the perturbative QCD contribution is much lower, say as predicted with the symmetric wave function, and one or more resonances is swamping the perturbative contribution. A 0^{-+} resonance would account for the isotropic angular distribution and the success of the $\gamma\gamma \rightarrow \pi^+\pi^-$ QCD predictions. (A 0^{-+} state cannot decay to a pair of pseudoscalars). If its mass were 2190 or 2350 MeV as mentioned above, it also would not contribute to $\gamma\gamma \rightarrow \Delta^{++}\bar{\Delta}^{++}$. The experimental level [3] of that reaction is near the symmetric-wave-function prediction (fig. 3). It would be extremely helpful to have the Born approximation predictions for the rest of the $\gamma\gamma \rightarrow B\bar{B}'$ reactions with sum-rule wave functions. The limit of ref. [3], $\sigma(\gamma\gamma \rightarrow \Delta^{++}\bar{\Delta}^{++})/\sigma(\gamma\gamma \rightarrow p\bar{p}) < 3$, is much smaller than predicted with the symmetric wave functions, and one might wonder if the sum-rule wave function for the Δ^{++} could manage to evade the naive value of (charge of the Δ^{++} /charge of the proton)⁴ = 16, for this ratio.

The most helpful experimental input we could have at this point would be the careful measurement of the energy dependence of the cross section: does it scale as s^{-5} for a fixed angular range as predicted, and can resonances be ruled out? Obviously, extending the energy to the $W_{\gamma\gamma} > 3$ GeV range would be extremely helpful. An accurate measurement of Δ^{++} pair production, combined with the theoretical prediction with the sum-rule wave function, may be a decisive test of the applicability of perturbative QCD to $\gamma\gamma \rightarrow B\bar{B}'$ in this $W_{\gamma\gamma}$ and t regime. Finally, further work is needed in the mesonic-pair final states to decide whether the perturbative QCD predictions [11] are really valid there: a 0^{-+} resonance could contribute to $\gamma\gamma \rightarrow \rho\rho$ and $\pi\rho$, so the QCD predictions should be studied there.

One of us (G.R.F.) would like to thank the Physics Department of Columbia University for its hospitality, and the John Simon Guggenheim Foundation for its support, during the completion of this work.

References

- [1] Ch. Berger, Proc. 1983 Int. Symp. on Lepton and photon interactions at high energy, Cornell, August 4–9, 1983
- [2] M. Althoff et al., Phys. Lett. 130B (1983) 449
- [3] M. Althoff et al., DESY preprint 84-015
- [4] S.J. Brodsky and G.P. Lepage, Phys. Rev. D22 (1980) 2157. (Note that the overall sign of the nucleon form factor Born amplitude given by Brodsky and Lepage is incorrect)
- [5] See A. Mueller, Phys. Reports for a review of perturbative QCD applied to exclusive processes and further references
- [6] G.R. Farrar, Phys. Rev. Lett. 53 (1984) 20
- [7] G.R. Farrar and F. Neri, Phys. Lett. 130B (1983) 109
- [8] P.H. Damgaard, Nucl. Phys. B211 (1983) 435
- [9] G.R. Farrar, E. Maina and F. Neri, Rutgers preprint RU-83-33, contribution to the 1983 Int. Symp. on Lepton and photon interactions at high energy, Cornell, August 4–9, 1983
- [10] G.R. Farrar, E. Maina and F. Neri, RU-84-13, QCD predictions for $\gamma\gamma$ annihilation to baryons
- [11] S.J. Brodsky and G.P. Lepage, Phys. Rev. D24 (1981) 1808
- [12] G.R. Farrar and D.R. Jackson, Phys. Rev. Lett. 43 (1979) 246
- [13] V.L. Chernyak and I.R. Zhitnitsky, Nucl. Phys. B246 (1984) 52
- [14] S.J. Brodsky, G.P. Lepage and P.B. Mackenzie, Phys. Rev. D28 (1983) 228
- [15] S.J. Brodsky and G.P. Lepage, Phys. Rev. D24 (1981) 2848
- [16] G.R. Farrar, Proc. VIth Int. Workshop on Photon-photon collisions, Lake Tahoe, CA, September 10–13, 1984, Rutgers Univ. preprint RU-84-19
- [17] S.J. Brodsky and G.R. Farrar, Phys. Rev. Lett. 31 (1973) 1153; Phys. Rev. D11 (1975) 1309
- [18] Alspector et al., Phys. Rev. Lett. 30 (1973) 511
- [19] Abrams et al., Phys. Rev. Lett. 18 (1967) 1209
- [20] Coupland et al., Phys. Lett. 71B (1977) 460